Nonlinear Topology Optimization of District Heating Networks: A benchmark of a Mixed-Integer and a Density-Based Approach

Yannick Wack[1,4,3], Sylvain Serra[2], Martine Baelmans[1,4], Jean-Michel Reneaume[2], Maarten Blommaert[1,4]

Abstract

The widespread use of optimization methods in the design phase of District Heating Networks is currently limited by the availability of scalable optimization approaches that accurately represent the network. In this paper, we benchmark two different approaches to nonlinear topology optimization of District Heating Networks in terms of computational cost and optimality gap. We compare a combinatorial approach, which directly solves a mixed-integer nonlinear program, against a density-based approach. This density-based approach relaxes the integer constraint on pipe placement and ensures near-discrete topologies through penalization. The benchmark shows subquadratic scaling of the computational cost for the density-based approach, making it tractable for large problems, while the combinatorial approach scales exponentially. The combinatorial approach took 29 hours to optimize a network for a neighborhood of about 600 streets, compared to 35 minutes for the density-based method. Optimality gap analysis indicates that resolving the integer constraint on pipe placement does not necessarily lead to a superior design, while making the optimization of large practical problems intractable. In contrast, the scaling of the density-based approach remains tractable for large problems. Further study of the optimality gap highlights the importance of consciously choosing initialization strategies when deciding to solve the nonlinear topology optimization problem.

Keywords: District Heating Networks, topology optimization, mixed-integer nonlinear programming, benchmark

1. Introduction

District Heating Networks (DHN) are considered one of the core technologies to enable carbon-neutral space heating [1]. It has the ability to connect a multitude of different renewable heat sources and provide heat to districts and entire cities. In DHNs, the typically high upfront investment cost of groundworks and piping is a core decision variable for the feasibility of a development project. Therefore in the planning phase it is crucial to design the pipe routing (network topology), pipe sizing and heat production capacities in an optimal way. This topology optimization problem solves the question of where to place heating network pipes and at what diameter, while accounting for the nonlinear nature of the heat transport physics. Together with the binary choice of pipe placement, it is therefore inherently a Mixed Integer Non-Linear Program (MINLP).

Directly solving this MINLP is often challenging and can become intractable for large problems. The literature on solving the topology optimiza-

Email address: `yannick.wack@kuleuven.be` (Yannick Wack)

[1]Department of Mechanical Engineering, KU Leuven, Celestijnenlaan 300 box 2421, 3001 Leuven, Belgium

[2]Universite de Pau et des Pays de l'Adour, E2S UPPA, LaTEP, Pau, France

[3]Flemish Institute for Technological Research (VITO), Boeretang 200, 2400 Mol, Belgium

[4]EnergyVille, Thor Park, Poort Genk 8310, 3600 Genk, Belgium

tion problem for DHNs can be classified into the following four main strategies:

- Heuristic methods.
- Combinatorial optimization directly solving the MINLP.
- Linearization creating a Mixed Integer Linear Program (MILP).
- Relaxation of the integer constraint, solving a Non Linear Problem (NLP).

Since the field of topology and design optimization of DHNs has expanded rapidly in recent years, examples of the four different approaches are reviewed in the literature. First, the use of heuristic search algorithms to solve the MINLP problem was done early on. Li and Svendsen [2] used a genetic algorithm to optimize the network topology based on a nonlinear thermal-hydraulic network model. To account for uncertainty, Egberts et al. [3] used a single objective genetic algorithm to optimize the topology and pipe diameters based on a heating network simulation. Allen et al. [4] used both a minimal spanning tree heuristic and a particle swarm algorithm to optimize the topology of a small DHN.

Fully exploiting the potential of mathematical optimization to solve the MINLP has been done notably by Mertz et al. [5]. They solve the full MINLP by directly resolving the discrete nature of pipe routing choices using a combinatorial optimization approach. This approach has been used to optimize the design of an existing DHN [6], and later by Marty et al. [7] for the optimal design of a Rankine cycle combined with a small heating network topology.

Both direct heuristic approaches and direct MINLP solutions are challenging and can become intractable for large problems. As a result, the topology optimization problem of heating networks is often linearized, resulting in a linear optimization problem that can be solved efficiently using MILP solvers. Söderman [8], for example, optimized the structure and configuration of a district cooling network using a MILP approach. Dorfner and Hamacher [9] later used a linear approach to optimize the topology and pipe sizes of a DHN. Haikarainen et al. [10] optimized the topology and operations, while accounting for different production technologies and heat storage. Mazairac et al. [11] optimized the topology of a multi-carrier network that incorporates gas and electricity supply. Morvay et al. [12] optimally designed the network while also optimizing the energy mix supplied. Using a MILP approach, Bordin et al. [13] optimized the network topology while studying the set of consumers to optimally connect to a DHN. Comparing a MILP formulation with a heuristic approach, Weinand et al. [14] optimize both the topology and the location of the heating plants. Neri et al. [15] used a linearized MILP approach to determine the optimal topology, pipe diameter, and set of consumers connected to a district cooling network. Similar to the previous authors, they compared this approach to heuristic methods, including a combination of a minimum spanning tree heuristic and a genetic algorithm. Recently, Resimont et al. [16] used a MILP approach to optimize a city-scale heating network. The transformation of modern DHNs towards multi-source, low-temperature networks [17] renders the assumptions of most linear heating network models inadequate. To accurately model heat losses and to account for different feasible temperature levels at both supply and demand sites in DHNs, a nonlinear representation of network physics is required. While linearized MILP approaches to the topology optimization problem of DHNs improve tractability, their applicability is therefore limited by the type of problems they can effectively solve.

An alternative way to improve tractability while preserving the nonlinear representation of network physics is to relax the integer constraint on pipe placement. This allows efficient solution of a NLP problem. Pizzolato et al. [18] used this method to robustly optimize the topology of a DHN based on a hydraulic network model. Later, Blommaert et al. [19] and Wack et al. [20] solved a relaxed NLP of the thermal-hydraulic problem, ensuring a discrete network topology through density-based penalization. The method is inspired by density-

based topology optimization, which is popular in the field of partial differential equation (PDE)-constrained topology optimization [21]. This method scales well with problem size, allowing optimization of large-scale problems.
The current bottleneck to a widespread use of optimization methods for the design and topology optimization of DHNs are an accurate representation of the network while maintaining scalability of the approach. Identifying the most suitable methods to address this challenge is crucial to facilitate the practical implementation of optimized DHNs. The goal of this paper is therefore to benchmark the performance of two methods for solving the nonlinear topology optimization problem of DHNs: the combinatorial approach by Mertz et al. [5] and the relaxed density-based approach by Wack et al. [20]. The benchmark analyzes the computational complexity of both approaches and compares their optimality gap to find the most promising method for future research. With this benchmark, we aim to streamline future research and potentially minimize redundant efforts. Therefore, we first compare the computational cost scaling of both optimization approaches with the network size to evaluate their suitability for large-scale DHN development projects. Both approaches solve nonlinear and non-convex optimization problems, so the found optimal network designs can be different local optima. Therefore, in a second step, the optimality gap between the two approaches is investigated for both single-producer and multi-producer DHNs. Here, the importance of resolving the discrete nature of the pipe routing problem, as well as the influence of initialization strategies on the found local optima is discussed.

2. The topology optimization problem of DHNs

To compare both approaches, a topology optimization problem is defined that aligns the problem definitions of Mertz et al.[5] and Wack et al [20]. This ensures comparability of the results with both approaches. For completeness, the optimization problem definition is repeated here in short, for detailed discussion the reader is referred to the afore-mentioned publications.

Table 1: Notation used to describe different subsets of the DHN.

Set	Symbol
All edges	E
Producer input	E_{pr}
Pipes	E_{pipe}
Feed edges	E_{f}
Heating system	E_{hs}

In order to represent the design and topology optimization problem of a DHN, a set of design variables $\boldsymbol{\varphi} = [\boldsymbol{d}, \boldsymbol{\gamma}]$ is defined, containing the pipe diameters $\boldsymbol{d}$ as well as the normalized producer inflows $\boldsymbol{\gamma}$. To represent the physical state of a given network, a vector of physical variables $\boldsymbol{x} = [\boldsymbol{q}, \boldsymbol{p}, \boldsymbol{\theta}]$ is defined. It contains the flow rates $\boldsymbol{q}$, nodal pressures $\boldsymbol{p}$ and nodal and pipe exit temperatures $\boldsymbol{\theta}$. The temperatures $\boldsymbol{\theta} = \boldsymbol{T} - T_\infty$ are defined as the difference between the absolute water temperature $\boldsymbol{T}$ and the outside air temperature T_∞. Now the topology optimization problem for a DHN can be posed as a generic optimization problem of the form:

$$\begin{aligned} \min_{\boldsymbol{\varphi},\boldsymbol{x}} \quad & \mathcal{J}\left(\boldsymbol{\varphi}, \boldsymbol{x}\right) \\ s.t. \quad & \boldsymbol{h}(\boldsymbol{\varphi}, \boldsymbol{x}) \leq 0. \end{aligned} \tag{1}$$

Here $\mathcal{J}$ represents the cost function and is defined as the total cost of the project over an investment horizon of $A = 30$ years. $\boldsymbol{h}(\boldsymbol{\varphi}, \boldsymbol{x})$ defines the set of model and technological constraints. A full definition of the cost function and model constraints for this benchmark can be found in Appendix A. This optimization problem is based on Mertz et al. [5] and Wack et al. [20] and a detailed description of the underlying costs and models can also be found there. In the problem definition, the set definition in table 1 is used to reference different parts of the network.

3. Methodology

To compare the two approaches, the topology optimization problem (described in equation 2) is solved using two different methods: solving the full MINLP problem in GAMS using the implementation of Mertz et al. [5] (referred to as fMINLP for simplicity), and using the density-based optimization approach of Wack et al. [20] implemented in the PATHOPT tool (referred to as pNLP). Both implementations were simplified to facilitate comparison. The pNLP implementation no longer considers multiple discrete pipe diameters, while the fMINLP implementation no longer optimizes the production side or cascading supply between high and low temperature consumers. The following sections briefly discuss the two methods and their different treatment of the binary pipe existence variable.

Combinatorial MINLP approach: fMINLP

For the comparison, the topology optimization problem will be solved using a combinatorial MINLP approach. This approach was previously published by Mertz et al. [5], and a comprehensive discussion of the approach can be found there. It is implemented in GAMS and uses the MILP solver CPLEX and the NLP solver CONOPT. To pose the optimization problem as a combinatorial problem, the topological choice of pipe placement is represented by a binary variable $\boldsymbol{\phi}$. Physical variables defined on these pipes are then coupled to this existence variable using the bigM method ($\mathcal{M}$) [5], as e.g. in the flow velocity definition:

$$m_{ij} - \mathcal{M}\left(1 - \phi_{ij}\right) \leq v_{ij}\rho\pi\frac{1}{4}d_{ij}^2 \tag{2}$$

$$v_{ij}\rho\pi\frac{1}{4}d_{ij}^2 \leq m_{ij} + \mathcal{M}\left(1 - \phi_{ij}\right), \quad \forall ij \in E_{\mathrm{pipe}}. \tag{3}$$

Here v denotes the flow velocity, and $\mathcal{M} \gg m_{ij}$ is chosen in such a way that if a pipe exists $\phi_{ij} = 1$, the bounds on the flow velocity constraint are tight. If $\phi_{ij} = 0$, the bounds of this constraints are relaxed. To force the installation of both feed and return pipes the following constraint is used:

$$\phi_{ij} = \phi_{ji}, \quad \forall ij \in E_{\mathrm{pipe}}. \tag{4}$$

The fMINLP implementation features additional constraints to facilitate convergence. They are defined in a way to not be active in the final optimal design, in order to maintain the same final problem formulation as the pNLP. First, the installed capacity H is bounded by the sum of the consumer demands:

$$\sum_{ij \in E_{\mathrm{pr,f}}} H_{ij} = \sum_{ij \in E_{\mathrm{pr,f}}} (q\theta)_{ij}\,\rho c_{\mathrm{p}} \leq 1.5 \sum_{kl \in E_{\mathrm{hs}}} Q_{kl}. \tag{5}$$

To facilitate convergence on the momentum equations, the velocity and pressure drop over a pipe are bounded by:

$$v_{ij} \leq 3.5, \tag{6}$$

$$v_{ij} \leq 18.438 d_{ij} + 0.2186, \tag{7}$$

$$v_{ij} \geq v_{\min}\phi_{ij}, \tag{8}$$

$$p_i - p_j \leq 200\,\mathrm{Pa} \quad \forall ij \in E_{\mathrm{pipe}}. \tag{9}$$

These constraints are not active in the final optimized design as they are dominated by the pipe momentum equation (A.8). A fixed pressure drop is set for the heat exchanger

$$p_i - p_j \geq 2\,\mathrm{kPa}, \quad \forall ij \in E_{\mathrm{hs}}, \tag{10}$$

and the exit temperature of the radiator is required to be smaller than the inflow temperature:

$$\theta_i \geq \theta_j, \quad \forall ij \in E_{\mathrm{hs}}. \tag{11}$$

Finally, this optimization strategy uses a sequence of initializations to ensure stable convergence of the final MINLP solve, based on the strategy of Marty et al. [7]. For completeness, this initialization sequence is briefly described in Appendix B.

Density-based penalization approach: pNLP

The other considered approach is the density-based penalization approach by Wack et al. [20]. Here, the combinatorial problem is relaxed, allowing for a continuous pipe placement choice. A near-discrete topology is then enforced by penalization, e.g. by replacing p_0 in the investment cost function (equation A.4) by

$$\bar{p}_0(d_{ij}) = p_0\left(\frac{1}{(1 + \exp(-k\left(d_{ij} - d_{\min}\right))} - 1\right), \tag{12}$$

or by explicitly penalizing the d in the investment cost function and within the momentum and energy equations, as described in Wack et al. [20]. Because of this relaxation, the MINLP reduces to solving a series of NLPs. Here the optimization is initialized with a uniform distribution of pipe diameters.

4. Benchmarking computational cost - a single producer case

Modern DHNs grow ever bigger and more complex, including multiple heat production sites at different temperatures, which optimal design tools must be able to handle. These tools therefore need to scale well with the heating network size in order to be applicable to relevant cases. In this first benchmark, the computational cost scaling of a combinatorial MINLP approach (fMINLP) is compared to solving a relaxed penalized NLP (pNLP). This is done on a benchmark case containing a single producer.

Setup

To be able to compare the computational cost scaling of both optimization approaches with increasing network size, an easily scalable DHN optimization case is set up. This benchmark case is visualized in figure 1.

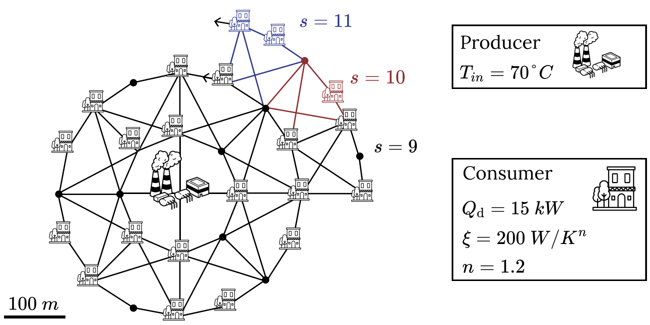

Figure 1: Setup of the first benchmark case. Around a central producer, heat consumers (houses) are arranged in a circular pattern. They are connected by possible pipe routes (black lines). Pipe junctions are visualized as black circles. To increase the size of this case, additional segments s are successively added to the outside of the network.

Here a heating network is to be designed around a single heat producer in the center of the network. This producer provides heat at 70 °C. Around this central producer, houses and possible pipe connections are arranged in a circular manner. All houses have a heat demand of $Q = 15\,\mathrm{kW}$, and their heating system characterized by $\xi = 200\,\mathrm{W/K}^n$ and $n = 1.2$. To investigate the cost scaling, the size of this circular network is successively increased by adding additional segments s. With each segment, additional heat consumers and 5 additional potential pipe connections are added, with the number of potential pipes following a linear scaling: $n(s) = 5s + 13$. In figure 1 the addition of the segments $s = 10$ and $s = 11$ is visualized in red and blue.

Now the benchmark of both approaches is performed by creating a series of heating networks of increasing size. Segments s are added in steps of 10, starting from $s = 0$ up to $s = 190$, thus creating a sequence of heating networks with $(s_k)_{k=0}^{19}$, $s_k = 10k$ segments. This sequence of optimization problems is solved by both the fMINLP implementation as well as the pNLP. This optimizations were performed on the same computer (using a single Intel Xeon 3.20 GHz processor core).

Comparison of the computational cost

The optimization was repeated 3 times for each network and the mean runtime until convergence (wall time) was recorded. The wall time for each network size is visualized in figure 2 on a a) semi-log graph and a b) log-log graph.

The figures show that the wall time for the fMINLP implementation scales faster with the network size then for the pNLP. The largest network size for which both approaches converged was $n = 612$ potential pipe connections. Here, the fMINLP approach took 28.75 hours to optimize the network, compared to 34.96 minutes using the pNLP. In order to get an understanding of how long it would take both approaches to optimize networks of considerable size, it is useful to understand which function governs their cost scaling. Considering the algorithmic differences of solving a MINLP in the case of the fMINLP and solving a relaxed NLP in the case of the pNLP, both an exponential and a polynomial time scaling were tested for both approaches. First, an exponen-

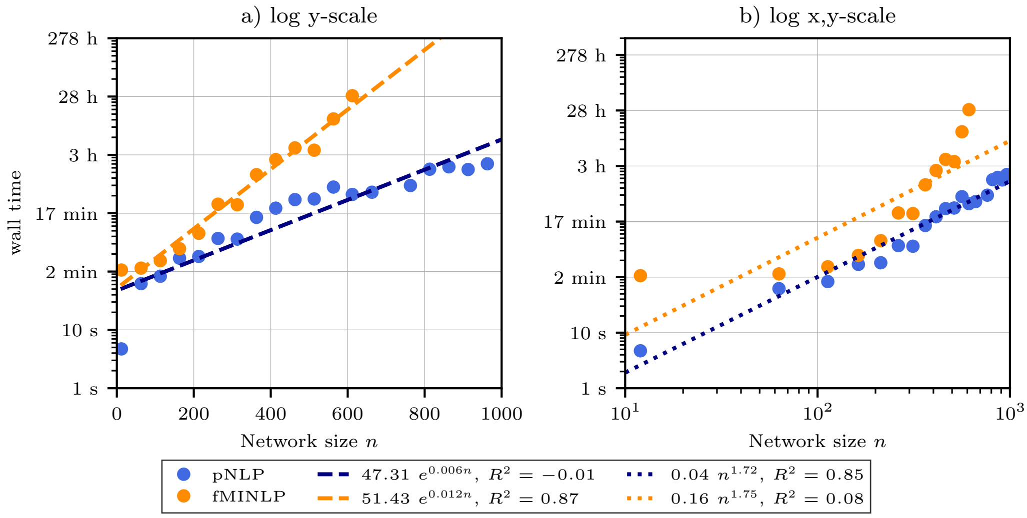

Figure 2: Wall time scaling of the two approaches with increasing network size n. The scaling of the approach in the fMINLP is described well by an exponential fit a), while the scaling of the pNLP can be described well by a power fit b). The pNLP did not converge for the case $n = 713$, while the fMINLP did not converge for any case $n \geq 663$. All non-converged optimizations are excluded from the figure and subsequent analysis

tial fit was performed for the scaling of both approaches (see figure 2 a)). The wall time scaling of the fMINLP can here be described by the function $w_{\text{fMINLP}}(n) = 51.43e^{0.012n}$ s with an coefficient of determination of $R^2 = 0.87$, while the wall time scaling of the pNLP can be described by $w_{\text{pNLP}}(n) = 47.31e^{0.006n}$ s with a coefficient of determination of $R^2 = -0.01$. From this fit it can be concluded that the wall time scaling of the fMINLP approach can be described well by an exponential function, while the wall time scaling of the pNLP approach cannot. Second, a power function was fitted to the wall time scaling of both approaches. Here, the scaling of the pNLP can be described by $w_{\text{pNLP}}(n) = 0.04n^{1.72}$ with a coefficient of determination of $R^2 = 0.85$ and the scaling of the fMINLP can be described by $w_{\text{fMINLP}}(n) = 0.16n^{1.75}$ with $R^2 = 0.08$. It can be concluded that the wall time scaling of the pNLP follows a polynomial function reasonably well, while the fMINLP cannot be described by a polynomial function.

The comparison above highlights the potential exponential solution time of solving full MINLPs. In the context of DHN optimization, this steep cost scaling does not only make design studies slow and expensive, its exponential nature renders optimizations of considerably sized networks intractable and serves as a bottleneck for the optimization of large-scale DHNs, containing thousands of potential pipe connections. For example to optimize a network containing $n = 2000$ potential pipe connections, an optimization time of $w_{\text{fMINLP}}(n) \approx 43000$ years would be needed extrapolating the observed exponential trend of the MINLP solution time. In the context of topology optimization of DHNs, it is computationally favorable to solve a relaxed NLP, as is evident from the polynomial wall time scaling of the pNLP implementation. The polynomial scaling of the computational solution time with this approach makes large-scale DHN optimization feasible. This is highlighted for the above example of a network with $n = 2000$, where the necessary optimization time reduces to $w_{\text{pNLP}}(n) \approx 5.3$ hours when using the relaxed NLP implementation of the pNLP, extrapolating the observed polynomial trend.

The potentially exponential computational cost scaling of solving full MINLPs should be taken into account when choosing optimization strategies for DHN topologies. It will make the optimization of large-scale DHNs intractable and hinder the application of such optimization tools to real-world DHN problems. It is therefore advisable to simplify the MINLP formulation by either linearizing the nonlinear model constraints, posing the problem as a MILP, or by relaxing the integer constraints, reformulating the problem as a NLP. This second relaxation is done within the pNLP implementation, and while keeping the nonlinear model in the overall optimization procedure, its significant speed-up in computational cost is shown in this paper.

Comparison of found optimal network topologies

Both approaches solve a nonlinear optimization problem. This is necessary because the nonlinear heat transport physics can have a large influence on the network design. Non-linearities in the optimization problem, however, can lead to multiple local optima. The proneness of both optimization approaches to these local optima is therefore studied in a next step. Here it can be investigated, if the relaxation of the integer constraints of pipe placement by the pNLP has a relevant influence on the cost of the found optimal network design. For this purpose, the optimality gap of both approaches is compared. The optimal total annualized cost for each benchmark step found with both approaches is visualized in figure 3.[1]
It can be seen that in this case the fMINLP implementation (figure 3 red) consistently finds a cheaper DHN design than the pNLP implementation (figure 3 blue). To check if this optimal design found by the fMINLP is indeed a better local optimum, the optimization is repeated in the pNLP and initialized with the optimal design found in the fMINLP (Figure 3 green). As can be seen in figure 3, the pNLP remains in the optimum of the fMINLP, indicating that it is indeed a better local optimum that the pNLP was unable to find with the used initialization strategy.
To better understand the difference in optimal network designs that causes this cost difference, the optimal network topologies found for network sizes $n = 63$ and $n = 463$ by both approaches are visualized in figure 4. The figure shows that

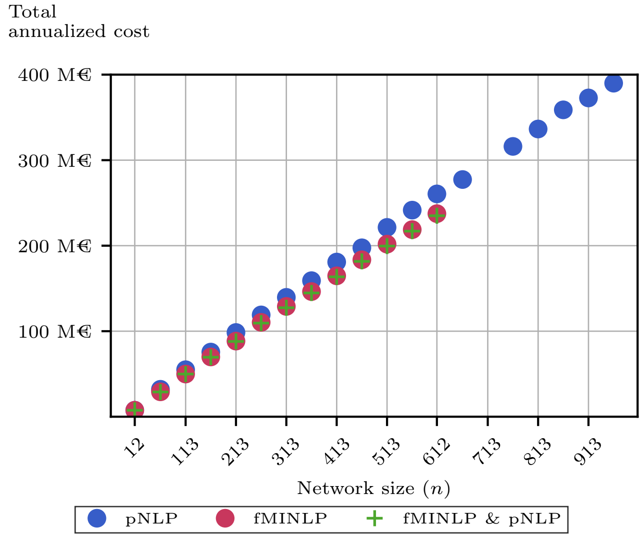

Figure 3: Comparison of the optimal total annualized cost for each benchmark step found by the fMINLP implementation (orange) and the pNLP implementation (blue). To verify that the fMINLP indeed consistently found a cheaper local optimum, the pNLP optimization is run using the fMINLP optima as initialization (green). The pNLP did not converge for the case $n = 713$, while the fMINLP did not converge for any case $n \geq 663$. All non-converged optimizations are excluded from the figure and subsequent analysis

the optimal topologies of both approaches differ, with the pNLP using overall a longer pipe length. This difference in the optimal design can be explained by the different initialization methods of the optimization approaches. To facilitate convergence, the fMINLP implementation is initialized with a MILP solve, that effectively minimizes the overall used pipe length while satisfying the heat demands of the consumers. This initialization promotes topologies with minimal pipe lengths, which turns out to be a good optimal network topology for single producer networks. This optimal topology continues to be an optimum when later solving the full MINLP as well, as can be seen in figure 4 b) and d). The pNLP, on the other hand, initializes the full MINLP from a uniform distribution of pipe sizes, and thereby finds a different local optimum with a larger overall pipe length (see figure 4). This knowledge of the influence of initializations on the optimal topology can be used to reduce the sensitivity to local optima for both optimization approaches. In the follow-

[1]To prevent potential remaining modelling differences from skewing the comparison, both found optimal designs where evaluated in a simulation within the pNLP.

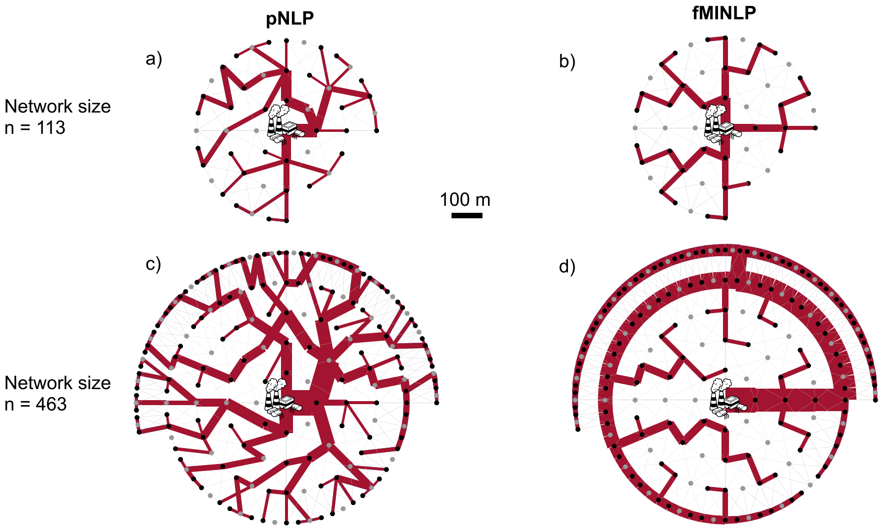

Figure 4: Comparison of the optimal topology found with the fMINLP and the pNLP for the case of size $n = 113$ and the case of size $n = 463$. The optimal topologies found by the fMINLP use a shorter pipe length then the topologies found by the pNLP. Red lines represent the pipe network connecting the producer, heat consumers (black dots) and pipe junctions (grey dots). The line thickness indicates the pipe diameter while unused pipe connections are drawn in grey.

ing section 5, it will be studied how the initialization of both approaches performs on a multi-producer case.

5. The influence of initialization - a two producer case

Modern 4th generation DHNs often feature multiple producers with different injection temperatures. To compare how both optimization approaches perform when designing such networks, a benchmark case was designed featuring two heat producers.

Setup

For this benchmark, a circular scalable test case with two producers with different injection temperatures is set up. The layout of this case is shown in figure 5. The circular network superstructure for this case is equivalent to the case in section 4, representing a potential district to be connected to a DHN. Here, two producers are placed to the left and right of this district. The two producers represent different heat production technologies, with the left producer supplying heat at 70 °C with high costs ($C_{\mathrm{hC}} = 800\,€/\mathrm{kW}$, $C_{\mathrm{hO}} = 8\,\mathrm{ct}/(\mathrm{kW\,h})$), while the producer on the right supplies heat with 55 °C at a lower cost ($C_{\mathrm{hC}} = 0\,€/\mathrm{kW}$, $C_{\mathrm{hO}} = 4\,\mathrm{ct}/(\mathrm{kW\,h})$). The district contains houses with different heat system characteristics. While the houses on the top right, using a modern heating systems, can work with water at $\gtrapprox 50\,°\mathrm{C}$, the rest of the houses require heat at higher temperatures ($\gtrapprox 60\,°\mathrm{C}$) than the low temperature producer can provide. The size of this network can be increased by adding additional rings of houses to this network, representing different sizes of DHN development projects.

Comparison of the optimized network designs

The presented case is now optimized using both the fMINLP and pNLP implementations. To compare the two approaches, three different networks of increasing size are optimized (case 1 with $n = 138$, case 2 with $n = 298$ and case 3 with $n = 618$). The annualized costs of the resulting optima found by both approaches are visualized in figure 6.[2]

The cost comparison shows that in this two producer case, the pNLP found an optimal network

[2] Again the optima of both approaches were evaluated with a pNLP simulation to avoid discrepancies.

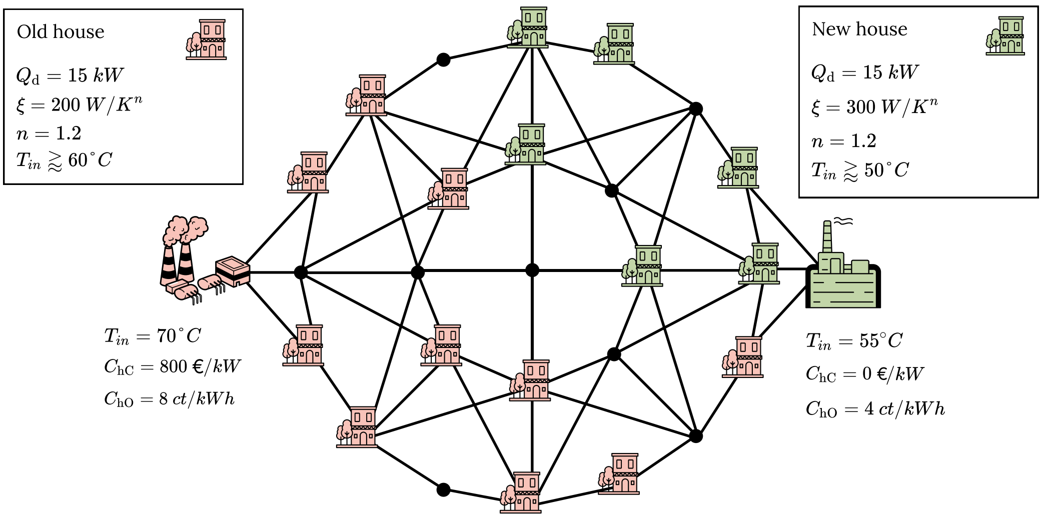

Figure 5: Setup for the two producers case. This setup features two producers on the left and right of a circular network. The network features old houses that require high temperature heat (red) and newer houses that can satisfy their demand with lower temperatures (green). The heat from the left producer (red) can supply all houses, while the right producer (green) can only supply the houses in the top right quadrant.

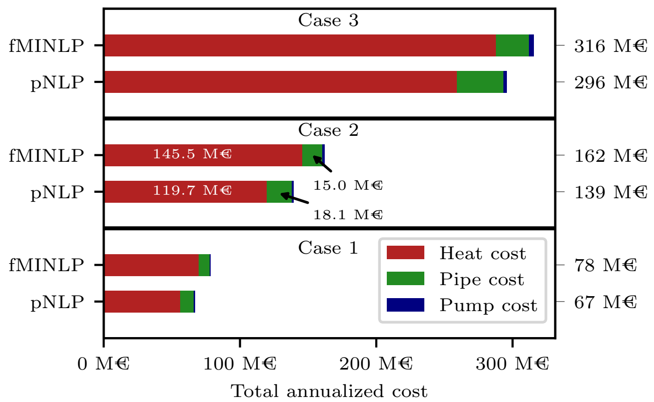

Figure 6: Comparison of the optimal total annualized cost for cases 1-3 found by the fMINLP and the pNLP implementations. While the fMINLP finds optimal design of lower pipe costs (green), the pNLP finds optimal designs that save on heating costs (red), ultimately leading to lower total annualized costs for all three cases.

design with a lower total annualized cost than the fMINLP in all three cases. While the optimal network design of the fMINLP is again cheaper in pipe investment cost, large savings in heat costs can be made with the proposed optimal design by the pNLP. While in case 2 the pipe investment cost of the optimal network design found by the fMINLP is 2.1 M€ lower, the optimal design found by the pNLP achieves heat cost savings of 14.4 M€, ultimately leading to a lower total annualized cost.

For a better understanding of the difference in the optimal designs, the optimal topologies of both approaches are compared. In figure 7, the optimal network topologies of cases 1 and 2, optimized by both the pNLP and the fMINLP, are visualized. It can be seen that the optimal topologies found by the pNLP connect most new houses to the low temperature producer on the top right, effectively creating two separate networks at different temperatures. This use of cheaper, low-temperature heat from the producer on the right leads to the cheaper optimal network designs in comparison to the fMINLP that where observed in figure 6. The initialization steps of the fMINLP[3], on the other hand, minimize pipe length while satisfying the heat demands. Therefore, the method favors an optimal topology for both cases that connects all houses to the high temperature producer on the left. The topology resulting from this initialization remains a local optimum also for the full MINLP optimization. While saving on pipe investment costs, this optimal network topology found by the fMINLP is more expensive than the optimal topology by the pNLP because it relies on buying more expensive, high-temperature heat

[3]Further described in Appendix B

from the producer on the left.
The results of the benchmarking study indicate that the initialization strategy has a significant impact on the optimal designs found by the topology optimization approaches for both the single- and two-producer cases. This dependence on initialization should always be taken into account when solving non-convex optimal design problems for DHNs that use nonlinear models or cost functions. The sensitivity to initialization could be mitigated by using global optimization, such as running multiple optimizations from different initializations, as demonstrated by Marty et al. [7].

6. Conclusion

In this paper, we compared the performance of two different approaches to the nonlinear topology optimization of DHNs. While the approach by Mertz et al. [5] solves a full MINLP, resolving the discrete nature of pipe routing choices using a combinatorial optimization approach (fMINLP), the approach by Wack et al [20] solves a relaxed NLP ensuring a discrete network topology through density-based penalization (pNLP).
First, by benchmarking the computational cost of both approaches, we showed that while solving the full fMINLP describes the routing choice more accurately, it has an exponential scaling of computational cost with network size. This exponential scaling renders optimizations of large networks containing thousands of potential pipe connections intractable. On the other hand, the relaxed pNLP approach maintains a polynomial scaling of computational cost, making large-scale DHN optimization feasible. In this benchmark, the fMINLP approach took 29 hours to optimize a network for a neighborhood of about 600 streets, compared to 35 minutes using the pNLP approach. We further highlighted the scaling difference of both approaches by showing that for a DHN featuring $n = 2000$ potential pipe connections, an optimization time of about 43000 years would be needed following the observed exponential trend of the MINLP solution time in the fMINLP implementation. The necessary optimization time reduces to about 5.3 hours when using the relaxed NLP implementation of the pNLP, assuming the observed polynomial trend.
This comparison of computational cost highlights the fact that full MINLP approaches may only be suitable for small problems, while relaxing the integer constraint is necessary for scalability. Despite the comparable scalability of linearized approaches (e.g., Resimont et al. [16]), this study did not benchmark against linear approaches due to significant differences in the types of problems that can be optimized. Future research should examine their performance relative to nonlinear methods to identify appropriate problems for which linear models are sufficient. In addition, our study did not benchmark heuristic methods, which could further contribute to a comprehensive understanding of the available optimization strategies for DHN topology problems.
Second, this benchmark investigated the optimality gap of both approaches. While posing the optimization problem as a nonlinear optimization problem has the benefit of an accurate representation of the DHN physics, Nonlinearities in the optimization problem can lead to multiple local optima. We showed in this paper how different initialization strategies can therefore lead to different optimal designs. The benchmark provided several examples of this. In a single-producer DHN case, the fMINLP implementation consistently outperformed the pNLP approach due to its focus on minimizing pipe length during initialization. This proved advantageous for single-producer networks. However, in a two-producer case, this strategy became a limitation, and the pNLP approach found more cost-effective network topologies. The comparison therefore showed that solving a full MINLP does not guarantee superior DHN topologies, while significantly increasing the computational cost.
In summary, this benchmark shows that while directly solving the MINLP may be suitable for small DHN topology optimization problems, its exponential computational scaling makes large practical network problems intractable. The benchmark also demonstrates that solving the discrete pipe placement constraint does not necessarily leads to superior network designs in the cases studied.

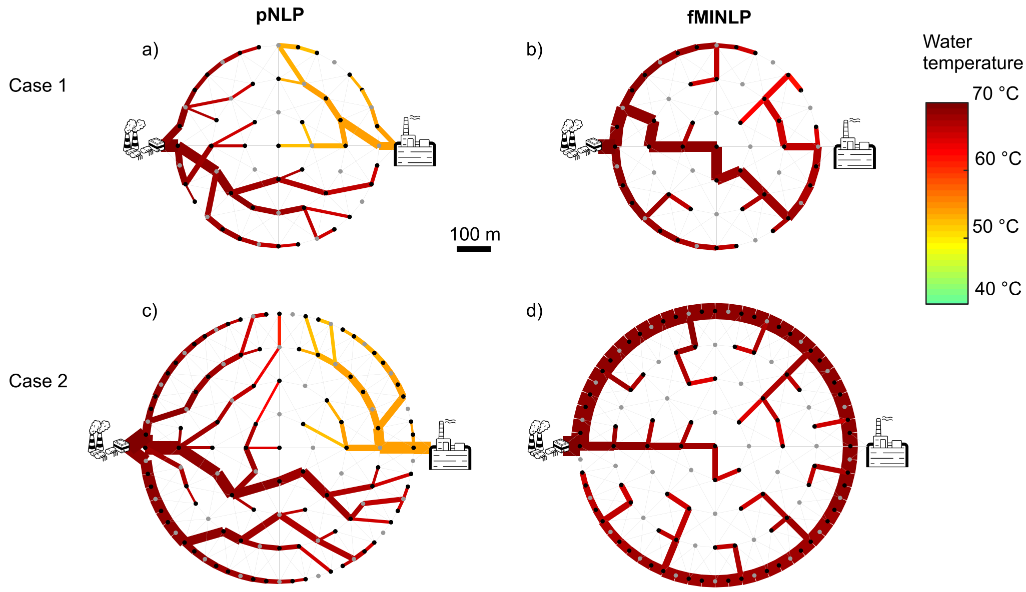

Figure 7: Colored lines represent the pipe network connecting the producer, heat consumers (black dots) and pipe junctions (gray dots). The line thickness indicates the pipe diameter, while unused pipe connections are drawn in gray. The line color corresponds to the water temperature in the pipe. While the pNLP finds an optimal topology connecting modern houses to the low temperature source, the fMINLP implementation favors a single network connecting all houses to the high temperature source.

For large topology optimization problems of modern DHNs, a density-based approach such as the pNLP approach studied here is therefore more appropriate. Finally, the benchmark also shows that the sensitivity to local optima and the consequent importance of initialization and initialization strategy should be taken into account when solving optimal design problems for DHNs using nonlinear formulations. It is important to formulate the routing problem in such a way that finding the global optimum is not a strict requirement, as long as an improved design is obtained, e.g., by starting a nonlinear optimization from an industry standard design (e.g., minimum spanning tree). This sensitivity to local optima could be mitigated by global optimization, such as running multiple optimizations from different initializations. Future studies should investigate the sensitivity of the found optimum to initialization for typical DHN routing problems to gain a comprehensive understanding of the solution space.

Data Availability

A data-set including the structure, input parameters and optimization results of the heating networks used in both benchmark cases of this paper is available at the following link: `https://doi.org/10.48804/DO1BRQ`. The optimization results can be replicated using the methodology and formulations described in this paper.
Additionally a small case generator was written that can be used to recreate all benchmark cases of this paper. The repository can be found at the following link: `https://doi.org/10.5281/zenodo.7434451`

Acknowledgements

A special thank you to Valentin Gressot for his support in aligning the software base of both approaches for the benchmark.
Yannick Wack is funded by the Flemish institute for technological research (VITO).

CRediT authorship contribution statement

Yannick Wack: Conceptualization, Formal analysis, Software, Visualization, Writing – original draft. **Sylvain Serra:** Conceptualization, Formal analysis, Software, Writing - Review & Editing. **Martine Baelmans:** Conceptualization, Writing - Review & Editing. **Jean-Michel Reneaume:** Conceptualization, Writing - Review & Editing. **Maarten Blommaert:** Conceptualization, Software, Writing - Review & Editing, Supervision.

Compliance with ethical standards

Conflict of interest
The authors declare that they have no conflict of interest

Funding
The authors did not receive support from any organization for the submitted work.

Ethical approval
This article does not contain any studies with human participants or animals performed by any of the authors.

Declaration of Generative AI and AI-assisted technologies in the writing process

Statement: During the revision stage of this work the authors used "DeepL Write" & "GPT" in order to improve readability and language of the text. After using this tools, the authors reviewed and edited the content as needed and take full responsibility for the content of the publication.

Appendix A. Detailed definition of the topology optimization problem for DHNs

In this section, the underlying cost function $\mathcal{J}$ and the set of model and technological constraints $\boldsymbol{h}(\boldsymbol{\varphi}, \boldsymbol{x})$ for this benchmark are defined in detail.

Appendix A.1. Cost function

The objective function is defined as the total cost of the project over an investment horizon of $A = 30$ years:

$$\begin{aligned}\mathcal{J}(\boldsymbol{\varphi}, \boldsymbol{x}) = & f_{\mathrm{CAP}}\left(J_{\mathrm{pipe,CAP}}(\boldsymbol{\varphi}) + J_{\mathrm{h,CAP}}(\boldsymbol{x})\right) \\ & + f_{\mathrm{OP}}\left(J_{\mathrm{h,OP}}(\boldsymbol{x}) + J_{\mathrm{p,OP}}(\boldsymbol{x})\right) , \end{aligned} \tag{A.1}$$

with

$$f_{\mathrm{CAP}} = (1 + e_{\mathrm{a}})^{A} , \tag{A.2}$$

$$f_{\mathrm{OP}} = \frac{1 - (1 + e_{\mathrm{a}})^{A} (1 + e_{\mathrm{i}})^{A}}{1 - (1 + e_{\mathrm{a}})(1 + e_{\mathrm{i}})} , \tag{A.3}$$

assuming a discount rate $e_{\mathrm{a}} = 0.04$ and an energy inflation rate $e_{\mathrm{i}} = 0.04$ [5]. The investment cost for the piping $J_{\mathrm{pipe,CAP}}$ is approximated with a linear interpolation of the catalogue cost of commercially available pipe diameters and the trench cost:

$$J_{\mathrm{pipe,CAP}}(\boldsymbol{\varphi}) = \sum_{ij \in E_{\mathrm{pipe}}} (p_1 d_{ij} + p_0) L_{ij} , \tag{A.4}$$

with $p_1 = 1976.3\,€\,\mathrm{m}^{-2}$, $p_0 = 301.4\,€\,\mathrm{m}^{-1}$ the interpolation coefficients and L the pipe length. The investment cost of the building heat production plants is calculated using

$$J_{\mathrm{h,CAP}}(\boldsymbol{x}) = \frac{\rho c_{\mathrm{p}}}{F \eta_{\mathrm{pr}}} \sum_{ij \in E_{\mathrm{pr,f}}} (C_{\mathrm{hC}}\, q\, \Delta\theta)_{ij} , \tag{A.5}$$

with the capacity price of heat production $C_{\mathrm{hC}} = 800\,€/\mathrm{kW}$, the capacity factor $F = 0.33$, and assuming an efficiency of $\eta_{\mathrm{pr}} = 0.9$. Here ρ is the density and c_{p} is the specific heat capacity of water. The operational heat cost is calculated using

$$J_{\mathrm{h,OP}}(\boldsymbol{x}) = \frac{\rho c_{\mathrm{p}}}{\eta_{\mathrm{pr}}} 8760 \frac{\mathrm{h}}{\mathrm{yr}} \sum_{ij \in E_{\mathrm{pr,f}}} (C_{\mathrm{hO}}\, q\, \Delta\theta)_{ij} , \tag{A.6}$$

with the unit price of heat $C_{\mathrm{hO}} = 0.06\,€/\mathrm{kWh}$. The operational cost of pumps at the heat production sites is computed with

$$J_{\mathrm{p,OP}}(\boldsymbol{x}) = \frac{8760}{\eta_{\mathrm{pump}}} \frac{\mathrm{h}}{\mathrm{yr}} \sum_{ij \in E_{\mathrm{pr,f}}} C_{\mathrm{pO},ij} (p_j - p_a) q_{ij} , \tag{A.7}$$

with the electricity price $C_{\mathrm{pO}} = 0.11\,€/\mathrm{kWh}$ and a pump efficiency of $\eta_{\mathrm{pump}} = 0.7$.

Appendix A.2. DHN model constraints

For all pipe junctions in the network, conservation of mass and energy is assumed.

Pipe model
The momentum equations in the pipes are modelled using the Blasius friction factor f, assuming a singular pressure drop of 30% [5]:

$$(p_i - p_j) = \frac{100}{70} f_{ij} \frac{8\rho L_{ij}}{d_{ij}^5 \pi^2} |q_{ij}| q_{ij}\,, \quad \forall ij \in E_{\text{pipe}}, \tag{A.8}$$

$$\text{with} \quad f_{ij} = 0.3164\,(Re)^{-\frac{1}{4}}\,, \quad \forall ij \in E_{\text{pipe}}. \tag{A.9}$$

Here Re is the Reynolds number, defined as $Re = \frac{4\rho|q|}{\pi\mu d}$. The energy equation over pipes is modelled accounting for the thermal conductivity of the pipe insulation $\lambda_{\text{i}} = 0.03\,\text{W}\,\text{m}^{-1}\,\text{K}^{-1}$ and the surrounding soil $\lambda_{\text{g}} = 1.4\,\text{W}\,\text{m}^{-1}\,\text{K}^{-1}$,

$$\theta_{ij} = \theta_i \exp\left(\frac{-L_{ij}}{\rho c_{\text{p}} |q_{ij}| U_{ij}}\right), \quad \forall ij \in E_{\text{pipe}}, \tag{A.10}$$

$$U_{ij} = \frac{\ln(4h/(r d_{ij}))}{2\pi\lambda_{\text{g}}} + \frac{\ln r}{2\pi\lambda_{\text{i}}}, \tag{A.11}$$

assuming an insulation ratio $r = 1.4$ and a pipe depth $h = 0.4\,\text{m}$ [19].

Consumer model
In the consumer arc, conservation of momentum is assumed. Conservation of energy in the heating system leads to

$$\rho c_{\text{p}} q_{ij}(\theta_i - \theta_{ij}) = Q_{ij}, \quad \forall ij \in E_{\text{hs}}, \tag{A.12}$$

with Q_{ij} the heat transferred to the house by the heating system. The latter is modelled with the characteristic equation for radiators [22] using the $LMTD$ approximation by Chen [23]:

$$Q_{ij} = \xi_{ij} \left(LMTD\left(\theta_i - \theta_{\text{house}}, \theta_{ij} - \theta_{\text{house}}\right)\right)^{n_{ij}}. \tag{A.13}$$

$$\text{with} \quad LMTD\left(\Delta\theta_{\text{A}}, \Delta\theta_{\text{B}}\right) \tag{A.14}$$

$$\approx \left(\Delta\theta_{\text{A}}\Delta\theta_{\text{B}}\left(\frac{\Delta\theta_{\text{A}} + \Delta\theta_{\text{B}}}{2}\right)\right)^{\frac{1}{3}}. \tag{A.15}$$

Here, θ_{house} is the inside temperature of the house, and ξ and n are heating system specific coefficients. The values of the coefficients ξ_{ij} and n_{ij} are tabulated for individual radiators, according to the EN 442-2 standard [24].

Producer model
At the producer, heat is injected with an input flow γ at a fixed temperature Θ:

$$q_{ij} = \gamma_{ij}, \quad \theta_{ij} = \Theta_{ij} \quad \forall ij \in E_{\text{pr,f}}. \tag{A.16}$$

Additional state constraints
To ensure that the heat demand $Q_{\text{d},ij}$ of every consumer is met, the following constraint is defined:

$$Q_{ij} - Q_{\text{d},ij} \geq 0\,, \quad \forall ij \in E_{\text{hs}}. \tag{A.17}$$

Appendix B. Initialization strategy of the combinatorial approach (fMINLP)

The initialization strategy for the MINLP approach is crucial for the overall solution process. The initial values for the variables and constraints in the MINLP model can greatly affect the solution's speed, accuracy, and feasibility. Figure B.8 shows the specific initialization strategy used in the fMINLP implementation.

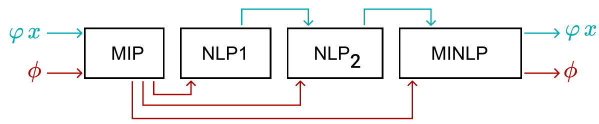

Figure B.8: Initialization strategy of the combinatorial approach (fMINLP). The optimal network topology ϕ determined by the MIP is used to initialize the following NLPs (red). The design variables $\boldsymbol{\varphi}$ and the physical variables $\boldsymbol{x}$ are optimized in a sequence of NLPs (blue).

The initialization strategy for the combinatorial fMINLP implementation consists of the following steps. In the first step (MIP), a MILP model is solved to determine an initial network topology. For simplicity, the nonlinearities present in the system are not considered. The optimal network topology of the MIP step is used in NLP_1,NLP_2 and the MINLP as the initial network topology (visualized by the red arrows in figure B.8). The first NLP model (NLP_1) is designed to consider some of the nonlinearities that were ignored in the initial MIP model. In this step, the characteristic equation of a radiator is used in a simplified form in order to reduce the computational complexity of the optimization problem. The second NLP model (NLP_2) takes into account the full set of nonlinearities present in the system. Finally, the full MINLP is solved including all constraints and binary variables.

References

[1] OECD/IEA, Renewables 2019 Analysis and forecast to 2024, Tech. rep. (2019).

[2] H. Li, S. Svendsen, District heating network design and configuration optimization with genetic algorithm, Journal of Sustainable Development of Energy, Water and Environment Systems 1 (4) (2013) 291–303. doi:10.13044/j.sdewes.2013.01.0022.

[3] P. Egberts, C. Tümer, K. Loh, R. Octaviano, Challenges in heat network design optimization, Energy 203 (2020) 117688. doi:10.1016/j.energy.2020.117688.
URL https://doi.org/10.1016/j.energy.2020.117688

[4] A. Allen, G. Henze, K. Baker, G. Pavlak, M. Murphy, An optimization framework for the network design of advanced district thermal energy systems, Energy Conversion and Management 266 (2022). doi:10.1016/j.enconman.2022.115839.
URL https://doi.org/10.1016/j.enconman.2022.115839

[5] T. Mertz, S. Serra, A. Henon, J.-M. M. Reneaume, A MINLP optimization of the configuration and the design of a district heating network: Academic study cases, Energy 117 (2016) 450–464. doi:10.1016/j.energy.2016.07.106.

[6] T. Mertz, S. Serra, A. Henon, J.-M. M. Reneaume, A MINLP optimization of the configuration and the design of a district heating network: study case on an existing site, Energy Procedia 116 (Suppl. C) (2017) 236–248. doi:10.1016/j.egypro.2017.05.071.

[7] F. Marty, S. Serra, S. Sochard, J.-M. Reneaume, Simultaneous optimization of the district heating network topology and the Organic Rankine Cycle sizing of a geothermal plant, Energy 159 (2018) 1060–1074.

[8] J. Söderman, Optimisation of structure and operation of district cooling networks in urban regions, Applied Thermal Engineering 27 (16 SPEC. ISS.) (2007) 2665–2676. doi:10.1016/j.applthermaleng.2007.05.004.

[9] J. Dorfner, T. Hamacher, Large-scale district heating network optimization, IEEE Transactions on Smart Grid 5 (4) (2014) 1884–1891.

[10] C. Haikarainen, F. Pettersson, H. Saxén, A model for structural and operational optimization of distributed energy systems, Applied Thermal Engineering 70 (1) (2014) 211–218. doi:10.1016/j.applthermaleng.2014.04.049.

[11] W. Mazairac, R. Salenbien, B. De Vries, Towards an optimal topology for hybrid energy networks, EG-ICE 2015 - 22nd Workshop of the European Group of Intelligent Computing in Engineering (2015).

[12] B. Morvaj, R. Evins, J. Carmeliet, Optimising urban energy systems: Simultaneous system sizing, operation and district heating network layout, Energy 116 (2016) 619–636. doi:10.1016/j.energy.2016.09.139.

[13] C. Bordin, A. Gordini, D. Vigo, An optimization approach for district heating strategic network design, European Journal of Operational Research 252 (1) (2016) 296–307.

[14] J. M. Weinand, M. Kleinebrahm, R. McKenna, K. Mainzer, W. Fichtner, Developing a combinatorial optimisation approach to design district heating networks based on deep geothermal energy, Applied Energy 251 (oct 2019). doi:10.1016/j.apenergy.2019.113367.
URL https://doi.org/10.1016/j.apenergy.2019.113367

[15] M. Neri, E. Guelpa, V. Verda, Design and connection optimization of a district cooling network: Mixed integer programming and heuristic approach, Applied Energy 306 (PA) (2022) 117994. doi:10.1016/j.apenergy.2021.117994.
URL https://doi.org/10.1016/j.apenergy.2021.117994

[16] T. Résimont, Q. Louveaux, P. Dewallef, Optimization Tool for the Strategic Outline and Sizing of District Heating Networks Using a Geographic Information System, Energies 14 (17) (2021) 5575. doi:10.3390/en14175575.
URL https://www.mdpi.com/1996-1073/14/17/5575

[17] H. Lund, P. A. Østergaard, T. B. Nielsen, S. Werner, J. E. Thorsen, O. Gudmundsson, A. Arabkoohsar, B. V. Mathiesen, Perspectives on fourth and fifth generation district heating, Energy 227 (2021) 120520. doi:10.1016/j.energy.2021.120520.

[18] A. Pizzolato, A. Sciacovelli, V. Verda, Topology Optimization of Robust District Heating Networks, Journal of Energy Resources Technology, Transactions of the ASME 140 (2) (2018) 1–9. doi:10.1115/1.4038312.

[19] M. Blommaert, Y. Wack, M. Baelmans, An adjoint optimization approach for the topological design of large-scale district heating networks based on nonlinear models, Applied Energy 280 (May) (2020) 116025. arXiv:2008.08328, doi:10.1016/j.apenergy.2020.116025.
URL https://doi.org/10.1016/j.apenergy.2020.116025

[20] Y. Wack, M. Baelmans, R. Salenbien, M. Blommaert,

Economic Topology Optimization of District Heating Networks using a SIMP-like Multi-Material Penalization Approach, arXiv (2022). arXiv:2205.12019v2, doi:10.48550/arXiv.2205.12019.

[21] J. D. Deaton, R. V. Grandhi, A survey of structural and multidisciplinary continuum topology optimization: Post 2000, Structural and Multidisciplinary Optimization 49 (1) (2014) 1–38. doi:10.1007/s00158-013-0956-z.

[22] Ashrae, Radiators, in: ASHRAE handbook, 2014, Ch. Radiators, p. 231. doi:10.1055/s-2008-1040325.

[23] J. J. Chen, Comments on improvements on a replacement for the logarithmic mean (jan 1987). doi:10.1016/0009-2509(87)80128-8.

[24] DIN, Radiatoren und Konvektoren – Teil 1: Technische Spezifikationen und Anforderungen; Deutsche Fassung EN 442-1:2014, Tech. rep., Deutsches Institut für Normung e. V. (2015).